

1 **Running Title:** Peroxisome-chloroplast tethering

2

3 ***Corresponding author:**

4 Imogen Sparkes

5 Biosciences,

6 University of Exeter,

7 Geoffrey Pope Building,

8 Stocker Road,

9 Exeter,

10 EX4 4QD,

11 UK

12 I.Sparkes@exeter.ac.uk

13 Tel: +44 (0)1392 723454

14

15 **Title:** *In vivo* quantification of peroxisome tethering to chloroplasts in tobacco
16 epidermal cells using optical tweezers

17

18 **Authors:** H. Gao¹, J. Metz^{1#}, N. A. Teanby^{2#}, A. D. Ward³, S. W. Botchway³, B.
19 Coles³, M. R. Pollard³, I. Sparkes^{1*}

20

21 **Affiliations:** ¹ Biosciences, University of Exeter, Geoffrey Pope Building, Stocker
22 Road, Exeter, EX4 4QD, UK

23 ² School of Earth Sciences, University of Bristol, Wills Memorial Building,
24 Queen's Road, Clifton, Bristol, BS8 1RJ, UK

25 ³ Central Laser Facility, Science and Technology Facilities Council, Research
26 Complex at Harwell, Didcot, Oxon OX11 0FA, UK

27

28 # Authors contributed equally

29 *corresponding author

30

31 **One sentence summary:** Optical tweezers shows that peroxisomes are strongly
32 tethered to chloroplasts, and more weakly to other unknown structures.

33 **Footnotes:**

34 IS and HBG are funded by the BBSRC (BB/I006184/2) and an STFC user access
35 facility grant (LSP907), JM is funded by a Wellcome Trust Institutional Strategic
36 Support Award (WT097835MF).

37

38 M.R. Pollard's current address, DFM A/S, K. Lyngby, Denmark 2800

39

40 I.Sparkes@exeter.ac.uk

41

42 **Abstract**

43 Peroxisomes are highly motile organelles that display a range of motions within a
44 short time frame. In static snapshots they can be juxtaposed to chloroplasts which has
45 led to the hypothesis that they are physically interacting. Here, using optical tweezers
46 we have tested the dynamic physical interaction *in vivo*. Using near-infrared optical
47 tweezers, combined with TIRF microscopy, we were able to trap peroxisomes and
48 approximate the forces involved in chloroplast association *in vivo*, and observed
49 weaker tethering to additional unknown structures within the cell. We show that
50 chloroplasts and peroxisomes are physically tethered through peroxules, a poorly
51 described structure in plant cells. We suggest peroxules have a novel role in
52 maintaining peroxisome-organelle interactions in the dynamic environment. This
53 could be important for fatty acid mobilisation and photorespiration through interaction
54 with oil bodies and chloroplasts, highlighting a fundamentally important role for
55 organelle interactions for essential biochemistry and physiological processes.

56

57

58 **Introduction**

59

60 A combination of genetically encoded fluorescent probes, advances in light
61 microscopy and interdisciplinary approaches have revolutionised our understanding of
62 organelle transport. Organelle movement in highly vacuolated leaf epidermal cells
63 appears erratic with individual organelles undergoing a range of movements within a
64 relatively short time frame; stop-go, change direction (trajectory) and can move at
65 varying speeds. Use of pharmacological inhibitors indicated a role for actin, and
66 therefore myosins in this process, however myosin-organelle specificity is poorly
67 characterised (Buchnik et al., 2015; Madison and Nebenführ 2013; Tamura et
68 al.,2013). We are therefore still at a relatively rudimentary stage in the understanding
69 of the molecular and physical control, and interaction of, organelles in plant cells
70 compared with that known in other model systems (Prinz 2014; Hammer and Sellers
71 2012). However, it is clear that organelle movement plays important roles in
72 physiological processes in plants; reduced movement effects growth and
73 development, and movement is correlated with responses to extracellular stresses such
74 as pathogens and heavy metals (see references in Madison and Nebenführ 2013,
75 Buchnik et al., 2015 and Sparkes 2011). Organelle interactions in other systems have

76 important roles in calcium and lipid exchange setting a precedent for physiologically
77 important roles in plants (Prinz, 2014). However, characterisation of the molecular
78 factors required to physically tether organelles as opposed to those which function in
79 the exchange of molecules at the interaction site is challenging. Monitoring organelle
80 interactions in highly vacuolated plant epidermal cells are further complicated by the
81 constraints imposed by the large central vacuole. Static snapshots provided through
82 electron microscopy of highly vacuolated cells, where the vacuole can effectively
83 ‘push’ organelles together giving the impression of direct interaction between
84 organelles, is not a suitable method to determine dynamic interactions. Other
85 techniques such as the laser induced shockwave by explosion method used by Oikawa
86 et al., (2015) works globally without directly manipulating the individual organelle.
87 Here, using optical tweezers with sub-micron precision, we provide a means to assess
88 and quantify the dynamic interaction between peroxisomes and chloroplasts *in vivo* in
89 leaf epidermal cells.

90

91

92 Peroxisomes are responsible for several biochemical reactions including the
93 glyoxylate cycle and β -oxidation which provides an energy source for germination in
94 oilseeds. They also produce and scavenge free radicals, synthesise jasmonic acid (JA),
95 IAA and are required for photorespiration (see references in Hu et al. 2012). The
96 photorespiratory pathway spans peroxisomes, chloroplasts and mitochondria where
97 phosphoglycolate produced in the chloroplast is converted back to 3-P-glycerate. It
98 has been suggested that functional connectivity between these organelles accounts for
99 the close association observed in ultrastructural micrographs (Fredericks and
100 Newcomb, 1969). Several *Arabidopsis pex10* (peroxisomal membrane protein)
101 mutants show altered chloroplast-peroxisome juxtaposition with a defect in
102 photorespiration while others do not (Schumann et al., 2007; Prestele et al., 2010).
103 Both Clumped Chloroplasts 1 (CLMP1) and Chloroplast Unusual Positioning 1
104 (CHUP1) encode for proteins that localise to the chloroplast, with CHUP1 playing a
105 role in cp-actin formation (Yang et al., 2011; Oikawa et al., 2003, 2008; Schmidt von
106 Braun & Schleiff 2008). Whilst CHUP1 and CLMP1 affect chloroplast positioning,
107 they have differential effects on peroxisome and mitochondrial location; *clmp1* causes
108 chloroplast clustering without affecting mitochondria or peroxisome location (Yang et

109 al., 2011), whereas *chup1* was reported to affect peroxisome location (Oikawa et al.,
110 2003). *In vitro* analysis through density centrifugation highlighted chloroplast
111 sedimentation with peroxisomes under certain conditions (Schnarrenberger and
112 Burkhard, 1977), although this does not necessarily reflect organelle interaction in
113 live cells. Peroxisome proteomics studies have been hampered by difficulties in
114 isolating pure peroxisomal fractions (Bussell et al., 2013). This could be indicative of
115 interaction, where associated membranes are isolated together, or ‘sticky’ non-specific
116 contaminating chloroplast membranes. The work by Oikawa *et al.* (2015) provides
117 insight into the physiological processes controlling peroxisome-chloroplast interaction
118 (photosynthetic dependent), but they did not determine the effective baseline force
119 required to move peroxisomes that were not next to chloroplasts under control or
120 altered environmental conditions. Comparisons between the relative forces required to
121 move peroxisomes next to chloroplasts versus those which are not next to chloroplasts
122 are critical in understanding and probing the physical interaction between the two
123 organelles; hypothesis being that tethering would increase the force required to move
124 peroxisomes compared to organelles which are not tethered. Since peroxisomes have
125 diverse biochemical roles that affect a wide range of physiological processes
126 throughout the plant life cycle (Hu et al. 2012), then an understanding of if and how
127 peroxisomes may interact with other subcellular structures is likely to be an important
128 consideration for efficient peroxisome function.

129

130

131

132

133 Peroxisomes are highly pleomorphic, dynamic organelles bounded by a single
134 membrane (Hu et al., 2012), whose movement is driven by acto-myosin dependent
135 processes (Jedd and Chua, 2002; Mano et al., 2002; Mathur et al., 2002; Avisar et al.,
136 2008; Sparkes et al., 2008). Tubular emanations termed peroxules (Scott et al., 2007)
137 can extend from the main peroxisome body, yet it is unclear what function they may
138 play. Formation is quite frequent in hypocotyl cells (Sinclair et al., 2009; Mano et al.,
139 2002; Cutler et al., 2000), can occur around chloroplasts in cotyledonary leaf
140 pavement cells (Sinclair et al., 2009), and do not always form from the trailing edge
141 of the peroxisome (Sinclair et al., 2009). Exogenous addition of hydroxyl ROS, or
142 exposure to UV light, induces peroxule formation (Sinclair et al., 2009). It has been

143 suggested that they represent increased surface area for increased biochemical
144 function, or might represent a morphological precursor for peroxisome division (Jedd
145 and Chua 2002). Based on subcellular co-alignment, a retro-flow model for potential
146 exchange of luminal content between the ER and peroxisome through the peroxule
147 has been suggested (Sinclair et al., 2009; Barton et al., 2013). However, these studies,
148 as with many others, interpret the close association between organelles to indicate
149 physical connectivity between organelles, whereas, in fact, in highly vacuolated leaf
150 epidermal cells organelles can be closely packed within the cytoplasm due to mere
151 spatial constrictions generated through the large central vacuole. This is further
152 complicated by the highly motile, and seemingly stochastic nature of acto-myosin
153 driven organelle movement resulting in frequent apparent organelle ‘collisions’ which
154 may not reflect a functional requirement for organelle interaction.

155

156 Optical trapping provides a highly specific and sensitive means to measure physical
157 connectivity between organelles. By focussing an infrared beam, it allows the user to
158 trap objects which have a significantly different refractive index to the surrounding
159 media. Upon trapping, the user can then move the trapped object relative to its
160 original position to gain an understanding of whether the movement affects the
161 position and motion of other structures (such as other organelles) which may be
162 physically attached to the trapped organelle. For example, unlike the ER, Golgi bodies
163 are amenable to trapping. By trapping and micromanipulating (i.e. precisely moving)
164 the Golgi, a physical association between the ER and Golgi was determined in a
165 qualitative manner (Sparkes *et al.* 2009b). Here, we have developed a system to
166 generate quantitative measures for organelle interaction by standardising and
167 automating how far we move the trapped organelle (which we call the translation
168 step) at a defined speed, and assessing how trapping efficiency alters in response to
169 the power of the laser trap itself. By using these parameters we can then model the
170 forces imparted on the organelle providing further insight into the tethering processes.
171 Our results indicate that peroxisomes are amenable to being trapped, that they
172 physically interact with chloroplasts in leaf epidermal cells, and surprisingly that
173 peroxisomes are also tethered to other unknown structures within the cell. This
174 approach therefore highlights that organelle interactions within plant cells are not
175 random but regulated through tethering. In addition we provide a novel role for

176 peroxules, and a simple biophysical model to describe peroxisome motion during the
177 trapping process.
178
179

180 **Results**

181

182 **Peroxisome association with chloroplasts is specific**

183

184 For organelles to interact they must move and physically ‘sit’ or reside next to one
185 another in a coordinated manner. To determine how peroxisomes move relative to
186 chloroplasts we observed both peroxisomes, chloroplasts and Golgi bodies within the
187 same tobacco leaf epidermal cell and assessed how long either peroxisomes or Golgi
188 resided next to chloroplasts. As organelles are physically constrained by the large
189 central vacuole and can be ‘pushed’ together, Golgi were monitored as they are not
190 functionally related to chloroplasts and so act as an inherent control. We observed that
191 the average residency time of peroxisomes was significantly higher than that of Golgi
192 bodies on chloroplasts; 1.46 ± 0.35 minutes (n=17) and 0.42 ± 0.05 minutes (n=51)
193 respectively t-test $p < 0.001$ (Supp movie 1). Due to these observations, and functional
194 connectivity through the photorespiratory pathway, we investigated whether
195 peroxisomes physically interact with chloroplasts *in vivo*.

196

197 **Peroxisomes are associated with chloroplasts in an actin independent manner**

198 In a motile system it is difficult to discriminate between physical tethering processes
199 between two organelles from acto-myosin driven events. We therefore assessed
200 whether interaction characteristics were actin dependent in the first instance. Note, the
201 concentration of latrunculin b used is sufficient to depolymerise actin and cause
202 cessation of organelle movement (Sparkes et al., 2009a; Sparkes et al., 2008).

203

204 The average percentage of chloroplasts with a juxtaposed peroxisome in the presence
205 or absence of actin (latrunculin b treated) were not significantly different from one
206 another; $22 \pm 5\%$ and $23 \pm 3\%$ respectively, t-test $p > 0.8$, data taken from 20 images
207 covering 0.4mm^2 leaf epidermal area. Using optical tweezers we then tested whether
208 these results indicated a peroxisome-chloroplast tethering mechanism in both motile
209 and non-motile (latrunculin b treated) samples. By trapping and subsequently moving
210 the peroxisome within the cell (Fig 1A-D) we observed that upon turning the trap off
211 the peroxisome recoiled back towards its place of origin irrespective of chloroplast
212 presence (Supp Movie 2B,C,D). This process has not been previously observed using
213 other techniques. On several occasions peroxules were observed from the trailing

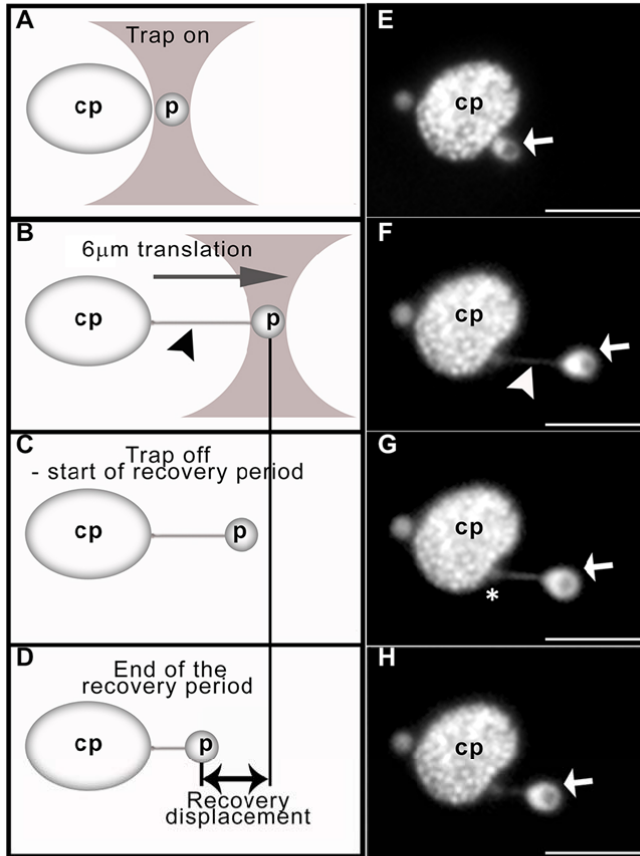


Figure 1. Optical trapping and movement of peroxisomes away from chloroplasts in tobacco leaf epidermal cells.

Schematic representation of the trapping procedure (A-D) and the corresponding micrographs (E-H) are shown. Upon turning the trap on (A,E) and moving the stage $6\mu\text{m}$ at a set speed (B,F; referred to as translation period) the trapped peroxisome (p, white arrow) is pulled away from the chloroplast (cp) and a peroxule (arrowhead) is formed. Upon turning the trap off (C,G) the peroxisome recoils back towards its original position next to the chloroplast (D,H). Peroxisome displacement during the recovery period (referred to as recovery displacement) is measured (double arrowhead). Asterisk denotes the tip of the peroxule. Scale bar $6\mu\text{m}$.

214 edge of the peroxisome (Supp Movie 2B,D). Upon actin depolymerisation, trapped
 215 peroxisomes displayed similar characteristics; peroxule formation and peroxisome
 216 recoil upon turning the trap off (Fig 1E-H, Supp movie 3A,B). These results indicated

217 that peroxisomes are tethered to chloroplasts and unknown structures in the cell, and
218 that peroxules may represent the site of tethering.

219

220 To test the hypothesis that peroxisomes are tethered to chloroplasts we set about
221 quantifying whether the average laser power required to trap and move peroxisomes
222 was dependent on chloroplast positioning and / or actin. The rationale here is that
223 trapping efficiency and movement are dependent on optical trap strength where
224 tethering, which acts as an opposing force, would impede the movement of the
225 trapped organelle causing it to escape the trap. Trapping refers to an organelle which
226 can be trapped and remains in the trap over the 6 μ m translation distance (Fig 1). Of
227 the fifty organelles from independent cells that underwent the trapping routine (which
228 constituted 5 samples of 10 organelles) there was a clear trend that increasing optical
229 laser power (from 24 to 50mW) resulted in an increase in the number of trapped
230 peroxisomes (20-38% increase) irrespective of actin or chloroplast association.
231 **However, peroxisomes which were next to chloroplasts were harder to trap.**
232 **Significantly fewer chloroplast associated (cp) peroxisomes were trapped** when
233 compared to non chloroplast (non-cp) associated peroxisomes under either motile or
234 immotile (latrunculin b treated) conditions at a given laser power; 50mW optical
235 trapping laser power resulted in average trapping of 38 \pm 2% cp and 56 \pm 7% non-cp
236 in the motile system, and 36 \pm 4% cp and 70 \pm 4% non-cp in the immotile system, t-
237 test p<0.05 comparing cp to non-cp under a given condition. These results indicate
238 that peroxisomes are tethered to chloroplasts and that this phenomenon is independent
239 of actin. The trapping efficiency of non-cp peroxisomes in the motile system
240 compared to the immotile system was significantly reduced (t-test p<0.15) and could
241 be due to a number of reasons; trapped peroxisome being knocked out of the trap by
242 passing organelles, docking the peroxisome onto actin filaments during the translation
243 or moving a trapped organelle into a cytoplasmic stream (Supp movie 2).

244

245 Peroxisome tethering can also be quantified by monitoring the recoil of the
246 peroxisome back towards its origin after turning the trap off (Fig 1, termed recovery
247 displacement). However, inherent difficulties of organelles escaping the trap and
248 responding to the acto-myosin driven elements after turning the trap off reduced the
249 number of organelles that could be assessed in this manner; for cp motile, and cp /

250 non-cp non motile system (latrunculin b treated) between 66-84% were measurable
251 compared with 21% for non-cp motile system. Observations of the small number of
252 organelles which showed recoil back towards the trap origin (recovery displacement,
253 Fig 1), rather than movement in an opposite direction in the motile system, indicated
254 that recoil was significantly larger for cp compared to non-cp in both motile and non-
255 motile conditions: for the motile system cp recovery displacement $3.92 \pm 0.36 \mu\text{m}$
256 (n=16) compared with non-cp recovery displacement $2.50 \pm 0.29 \mu\text{m}$ (n=6) $p < 0.007$;
257 for the non-motile system cp recovery displacement $3.65 \pm 0.45 \mu\text{m}$ (n=14) compared
258 with non-cp recovery displacement $1.22 \pm 0.20 \mu\text{m}$ (n=23) $p < 0.001$. All data were
259 taken using 50mW trapping laser power with a 5.3 second recovery period.

260

261 **Quantifying the peroxisome-chloroplast tethering process: a novel role for** 262 **peroxules**

263

264 The above observations clearly indicate that peroxisomes are tethered to chloroplasts,
265 and that this phenomenon is independent of actin. To further characterise the effects
266 of tethering, the opposing forces generated by the acto-myosin component were
267 removed from the system (latrunculin b treatment). Here, we assessed (1) the
268 relationship between peroxisome behaviour in the trap and trapping laser power over
269 a larger range of laser powers, and (2) behaviour of displaced peroxisomes after
270 turning the trap off (Fig.1,2). All of these observations were carried out under
271 latrunculin b treatment so that any interactions are due to tethering and not the acto-
272 myosin system.

273

274 Peroxisomes were either trapped, not trapped or escaped the trap during translation
275 (Fig 2c; movie S3C-E). As expected, the trapping laser power correlated with the
276 observed percentage trapping for both cp and non-cp peroxisomes (Fig.2A, B).
277 However, at laser powers of 37 mW and above there was a significant difference
278 between the trapping of cp and non-cp peroxisomes, with cp peroxisomes escaping
279 the trap more readily and non-cp peroxisomes being trapped and remaining in the trap
280 over the $6 \mu\text{m}$ translation (Fig 2, Supp Fig 1). Taken together this is indicative of more
281 force being required to trap and move peroxisomes away from chloroplasts.
282 Additionally, upon turning the trap off, cp trapped peroxisomes underwent a

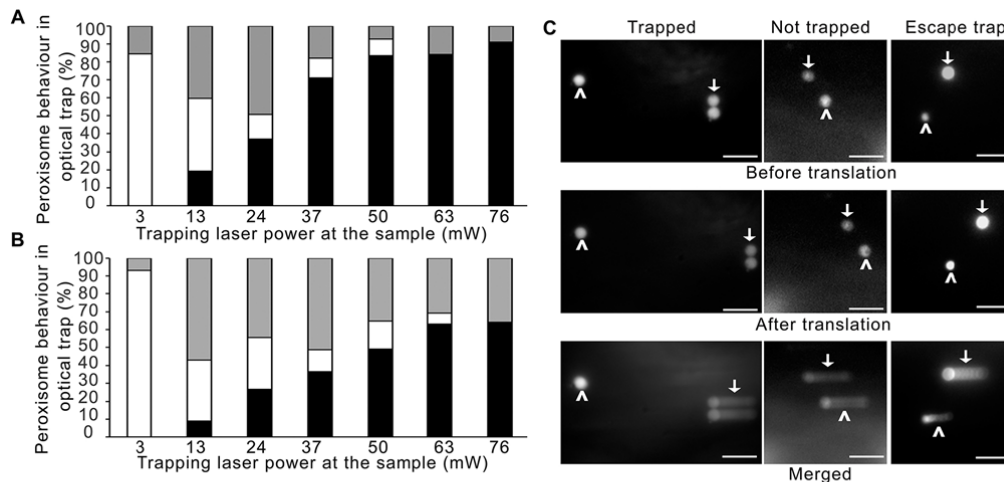


Figure 2. Higher optical trapping laser power is required to trap and move peroxisomes away from chloroplasts.

Non-cp (A) and cp (B) associated peroxisomes underwent the optical trapping protocol using various trapping laser powers and their trapping characteristics were scored; remained in the trap over the 6 μ m translation (black bar A,B), unable to be trapped (white bar A,B) or escaped the trap during the translation (grey bar A,B). Percentages displayed are based on weighted means from a set of independent experiments. Supp Figure 1 compares cp with non-cp for all three trapping categories and indicates significant differences between peroxisomes that are trapped or escape from the trap for cp versus non-cp. Relationship between optical laser trap power and peroxule formation are given in Supp table 1. Stills from Supp movie 3C-E representing before and after translation events for peroxisomes which are trapped, not trapped or escape the trap during the translation event are displayed (C, arrowhead). Note, peroxisomes not subjected to trapping in the same cell are shown for comparison (arrow). The translation event is based on movement of the stage and not the trap. Composite image of frames captured during the translation event show that the trapped peroxisome does not appear to move whereas organelles that escape the trap or are not trapped result in comet like tails (merged panels). Scale bar 6 μ m.

283 significantly larger recovery displacement (i.e. recoil, Fig 1D) than non-cp trapped
 284 organelles: cp recovery displacement $4.39^{+0.17}\mu\text{m}$ (n=94), non-cp recovery
 285 displacement $2.93^{+0.17}\mu\text{m}$ (n=91) using a laser power of 37mW, which has a t test
 286 probability value of $p < 0.001$. This proves that peroxisomes are tethered to
 287 chloroplasts *in vivo* in tobacco leaf epidermal cells. The above data were generated
 288 under a long recovery period (21.5 seconds rather than 5.3 seconds) to allow
 289 organelles to reach their equilibrium position, which improves the accuracy of the
 290 force determination discussed later.

291
 292

293 Peroxule formation can occur upon exposure to the trapping laser prior to and during
 294 the translation, however the frequency of formation is independent of the power of the
 295 optical trapping laser indicating that formation is not solely due to exposure to the
 296 trapping laser (Supp. table 1). Interestingly, both cp (38% n=170) and non-cp (37%

297 n=183) peroxisomes had a similar propensity to form peroxules, but the relative
298 percentages between formation in response to exposure to optical trap versus
299 translation differed (Supp table 1). It is unclear why more peroxules would form in the
300 absence of chloroplast positioning prior to translation (2.9% compared with 12%), but
301 we speculate that formation may occur in response to stress which is ameliorated by
302 the antioxidant properties of the chloroplast (Sinclair et al., 2009; Asada 2006), or
303 non-cp peroxisomes are tethered to structures whose positioning alters in response to
304 trapping the peroxisome.

305

306 During peroxisome translation peroxule formation is more frequent in cp versus non-
307 cp associated peroxisomes (28.2% compared with 15.3%, table S1), correlative with
308 peroxules being the visible manifestation of the tether to chloroplasts. The tip (point
309 of origin; see Fig 1G asterisk) of peroxules moved less during the translation process
310 in cp versus non-cp association, indicative of an anchored tether; cp $1.85^{+0.3}\mu\text{m}$
311 (n=37), non-cp $2.35^{+0.2}\mu\text{m}$ (n=46). In comparison, during the recovery period
312 peroxule tip displacement was much smaller, with values for cp and non-cp being
313 similar; cp $0.89^{+0.2}\mu\text{m}$, non-cp $1.13^{+0.1}\mu\text{m}$. If the base of the tether (i.e.
314 peroxule tip; see Fig 1G asterisk) is anchored, one would expect a higher level of
315 peroxisome movement (i.e. recoil) during the recovery period to correspond with a
316 lower level of peroxule tip movement during the translation; unlike non-cp samples,
317 there is a cluster of cp samples indicative of such behaviour suggesting strongly
318 anchored tether bases (Fig. 3).

319

320 **Biophysical modelling of peroxisome recoil indicates differences in relative forces** 321 **for peroxisome interactions**

322

323 Since both cp and non-cp peroxisomes exhibit different trapping (Fig. 2) and recovery
324 (Fig. 3) behaviours, we sought to understand the forces involved in this process;
325 specifically is it only the recoil distance which changes or are there changes in the
326 tether properties between cp and non-cp peroxisomes? To allow us to distinguish
327 between tether properties and changes in recoil distance we used a simple viscously
328 damped spring model to estimate the tether stiffness (i.e. spring constant) and tether
329 tension forces (i.e. initial recovery force) involved in the recovery process (Fig 4,

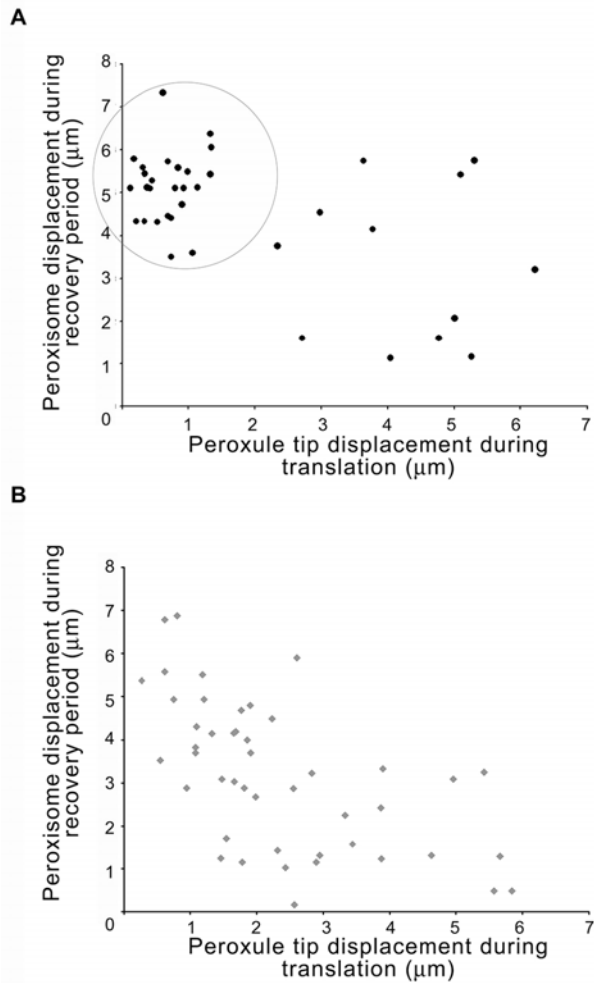


Figure 3. Correlation between peroxisome displacement during the recovery period and peroxule tip displacement during translation indicates anchored tethering between chloroplasts and peroxisomes.

Peroxisome tip displacement during the translation period was plotted against the peroxisome displacement during the recovery period for chloroplast associated (A; n=37) and non associated peroxisomes (B; n=46). Peroxisomes were trapped with 37mW optical trap laser power followed by a 21.5 second recovery period. The behaviour of cp samples is indicative of anchored tethers where the peroxule tip represents the base of the tether: small peroxule tip displacement combined with large peroxisome recovery displacement (circle). Note, the sample sizes are different to those in supplementary table 1 as displacement could only be measured if the peroxule was observable for the entire period.

330 Supp. note, Supp Fig 2-4). This first approximation indicates that tether stiffness
 331 values are similar for non-cp and cp (Fig 4B,C) and that differences in the recovery
 332 forces are solely due to the more rigid anchoring of cp associated peroxisome tethers,
 333 which leads to greater tether extension and subsequently greater recovery

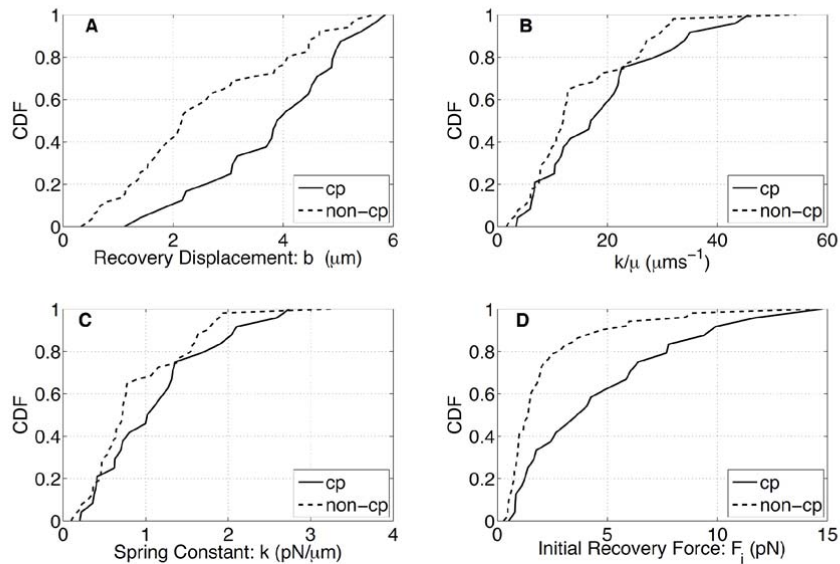


Figure 4. Cumulative distribution functions of model parameters for cp and non-cp associated peroxisomes.

Recovery displacement b is larger for cp than non-cp peroxisomes (A), whereas k/μ values, indicative of the tether stiffness, are broadly similar (B). Also, shown are the derived spring constants (C) and initial recovery forces (D) calculated assuming a viscosity of 0.06 Pa s for the cytoplasm. Values are derived using the spring model described in the supplementary information alongside Supp Fig 2-4.

334 displacement and initial recovery forces (Fig 4). In other words the biological
 335 structure that forms the tether between cp and non-cp peroxisomes behaves in a
 336 similar manner (i.e. similar stiffness), but the base of the tether (i.e. anchor point)
 337 moves less for cp peroxisomes thus generating more tension during translation and
 338 resulting in greater recoil. Here, non-cp peroxisomes are tethered to a structure which
 339 has greater mobility than chloroplasts during the trapping routine, so that upon
 340 moving non-cp peroxisomes, the tethered structure is also able to move to a certain
 341 extent resulting in lower tension ‘build up’ during the translation process. As we
 342 cannot independently estimate cytoplasmic viscosity in our system, this approach can
 343 only be used to determine relative differences in forces between cp and non-cp
 344 associated peroxisomes. However, using a reasonable value of 0.06 Pa s (Scherp and
 345 Hasenstein 2007) gives tether stiffnesses of $\sim 1\text{pN}/\mu\text{m}$ and initial recovery forces of
 346 $\sim 1\text{-}4\text{pN}$ (median values from Fig 4).
 347
 348
 349
 350

351 **Discussion**

352

353 By using optical tweezers we clearly show that peroxisomes can be tethered to
354 chloroplasts, and that relative differences in tethering strength highlight additional
355 subcellular interactions. Moreover, these tethers can be observed in several instances
356 as peroxules (Supp movie 2, 3). Such tethers are not solely restricted to chloroplast
357 interaction, but are also prevalent on non-cp peroxisomes (Supp movie 2, 3). In the
358 latter case, the tether interaction is either unstable or the structure it is tethered to is
359 more readily motile, accounting for the movement of the peroxule tip base during
360 translation. The mechanism of peroxule formation and extension is unclear, but the
361 rapid rate of extension makes *de novo* synthesis unlikely. Alternatives could be that
362 the bounding membrane itself is deformable, or that peroxules are tightly coiled
363 around the peroxisome and indistinguishable from the fluorescence signal arising
364 from the lumen of the main peroxisome body. It is unclear if the connectivity between
365 peroxisomes and chloroplasts is direct or indirect as positioning could be mediated
366 through interaction with the ER. The ER forms a basket around the chloroplasts
367 (Schattat et al., 2011), and *in vitro* optical trapping data inferred a chloroplast-ER
368 connection in Arabidopsis and pea leaf cells (Andersson et al., 2007). Peroxisomal
369 membrane protein Pex3p has been implicated in acting as a direct tether between the
370 ER and peroxisomes in *S. cerevisiae* (Knoblach et al., 2013). However, the complex
371 biogenetic link between peroxisomes and the ER has been, and continues to be,
372 debated within the community (Hu et al., 2012). Our previous observations of ER
373 responses upon trapping and moving Golgi highlight that a large percentage of the ER
374 is freely mobile, however chloroplast-ER interactions were not investigated (Sparkes
375 et al., 2009b). Therefore, if chloroplast-peroxisome connectivity is mediated by an ER
376 bridge, then perhaps the ER is highly constrained around chloroplasts which could
377 lead to greater recoil of trapped cp peroxisomes compared with non-cp cases. This is
378 an area of future study requiring further development of the imaging system. Using
379 the approaches developed here, future studies will enable the molecular and
380 physiological consequences of peroxisome-organelle interaction to be studied, and
381 could also be used to study the formation of membrane extensions.

382

383 Interactions between organelles are likely required for communication and transport.
384 Examples in yeast and mammals infer a requirement for lipid and calcium exchange

385 (Prinz 2014). In plants reports for ER-Golgi (Sparkes et al., 2009b), nucleus-plastid
386 (Higa et al., 2014), ER-chloroplast (Andersson et al., 2007; Mehrshahi et al., 2013),
387 peroxisome-oil body (Thazar-Poulot et al., 2015) interactions have been made, along
388 with a recent report from Oikawa *et al.* (2015) inferring a chloroplast-peroxisome
389 interaction in *Arabidopsis mesophyll* cells. This study, along with previous reports,
390 indicates peroxisomes undergo light dependent morphological changes (Desai and Hu
391 2008;Oikawa et al., 2015). Furthermore, by effectively inducing a localised
392 intracellular shock wave, Oikawa *et al.* inferred light, and photosynthesis, dependent
393 connections between peroxisomes and chloroplasts. Here, using a complementary
394 approach we trap individual peroxisomes in tobacco leaf epidermal cells, and
395 additionally compare the responses between chloroplast associated and non-associated
396 peroxisomes. Our results provide a clear indication of interaction of peroxisomes with
397 chloroplasts, and other unknown structures, and we provide a biophysical model for
398 the forces involved in the tethering process. We have also visualised the tethering
399 process through peroxule production, observations which were not made in the work
400 of Oikawa *et al.* and therefore suggest a novel role for peroxules in maintaining
401 physical connectivity between peroxisomes and the structure(s) to which it is tethered
402 to. The two techniques infer forces for the peroxisome-chloroplast interaction, but by
403 the very nature of the techniques the forces relate to **different biological aspects of the**
404 **interaction**; Oikawa *et al.* models the force required to push the two organelles apart
405 (**23-61 fN nm⁻²**), whereas here we model the forces imparted on the organelle after
406 they have been separated. It is important to note that the speed used to separate the
407 organelles using optical tweezers is within the range of reported peroxisome speeds in
408 an unperturbed system (Sparkes *et al.* 2008), and so cytoplasmic viscosity will affect
409 interactions in a way in which reflects the native motile system. Whereas the force
410 imparted on peroxisomes using the focused femtosecond laser technique was reported
411 to be so large that the effects of cytoplasmic viscosity would not hinder free
412 peroxisome motion, and are therefore negligible in their system. We do not infer a
413 precise force for trapping and moving the organelle (as viscosity values are currently
414 unknown for the system) and so compare the trapping profiles of chloroplast
415 associated and non-associated peroxisomes in response to the trapping laser power.
416 Both systems therefore provide different force components and have different
417 strengths and weaknesses in assessing the peroxisome-chloroplast interaction.
418 Furthermore, the basic spring model provides a baseline for interactions and will be

419 useful in testing how effective tension and stiffness change under altered
420 environmental conditions that may regulate the interaction between peroxisomes and
421 chloroplasts. For example, as photorespiration and photosynthesis may affect
422 interaction, does the rate of recoil of a trapped peroxisome change indicating a
423 ‘tighter’ tethering process between peroxisomes and chloroplasts or other structures
424 within the cell, and does this altered response affect tether stiffness rather than
425 tension?

426

427 Several organelles in plant cells produce tubular emanations; stromules, matrixules
428 and peroxules extend from chloroplasts, mitochondria and peroxisomes respectively
429 (Scott et al., 2007; Mathur et al., 2012; Hanson and Sattarzadeh 2013). Mapping
430 stromule dynamics, and the movement of protein and small molecules lend support to
431 a role in communication. However, contradictory data from different groups on
432 molecular exchange between stromules makes this an interesting and contentious area
433 of research (Hanson and Sattarzadeh 2013; Mathur et al., 2013). Here, our results
434 infer a similar role in communication, and we propose that tubular emanations are a
435 consequence of organelles attempting to maintain connections in the highly dynamic
436 intracellular environment. Peroxule formation occurs in response to hydroxyl reactive
437 oxygen species (ROS) with a concomitant reduction in peroxisome speed (Sinclair et
438 al., 2009). This could be interpreted as a response to maintain connections between
439 peroxisomes and another organelle whose motility has not been affected, or has been
440 increased during this treatment, effectively increasing the spatial separation between
441 the two organelles. Whilst the biophysical model provided herein reveals pN force
442 measurements imparted on the organelle during the recovery process, it also gives an
443 indication of the force required to pull the organelle micron distances. Here, the motor
444 force to separate organelles is expected to be the same or greater than the force
445 required for the organelles to be ‘pulled’ back towards their resting position (i.e.
446 referred to as the restorative force in the biophysical model). This approach could
447 therefore determine how motor regulation is controlled in order to maintain
448 peroxisome movement under conditions where interaction with chloroplasts is up /
449 down regulated.

450

451 Organelle movement plays important roles in growth, development and in response to
452 (a)biotic stresses (see references in Madison and Nebenführ 2013, and Buchnik et al.,

453 2015). In a wider context, the results presented herein allow us to start to bridge the
454 interface between organelle movement and interaction, and the forces involved in
455 these processes. Whilst future studies are required to validate the force measurements
456 with known cellular viscosities, in broader terms, these studies demonstrate that
457 interactions between organelles such as peroxisomes and chloroplasts in plant cells
458 are not random, but are controlled through tethering mechanisms which can be
459 quantified using optical tweezers. Regulation of organelle interaction / association
460 will be controlled by motor driven movement to position organelles next to one
461 another to allow tethering processes to occur. The force balance between these two
462 processes therefore needs to be viewed in conjunction to describe organelle motion
463 and positioning. Organelle interactions in plants could be required for communication
464 and so future studies pinpointing the tethering and motor components could provide a
465 novel way in which to control subcellular communication.

466

467

468

469 An interdisciplinary approach will be needed to fully characterise the molecular and
470 physiological role(s) of peroxisome-chloroplast interactions, and interactions with
471 other unknown organelles which could include lipid bodies. Current evidence points
472 towards photosynthetic dependent processes and a role for PEX10 in peroxisome-
473 chloroplast interactions (Oikawa et al., 2015; Schumann et al., 2007; Prestele et al.,
474 2010). It will also be interesting to assess what role ROS signalling may play in these
475 interactions (Sandalio and Romero-Puertas, 2015), and whether the exchange of
476 additional small molecules such as IAA and JA may be facilitated by organelle
477 interaction. Future genetic screens and proteomic approaches will pinpoint the
478 complex of proteins necessary for interaction. The essential domains required for
479 tethering will be mapped using biophysical means, such as optical tweezers, to
480 quantify effects on peroxisome-chloroplast / organelle interaction. Ultimately, the
481 analysis of resulting lines deficient in the tethering process will provide both
482 molecular, biochemical and physiological evidence for the role of peroxisome-
483 chloroplast / organelle interaction.

484

485

486

487 **Methods**

488

489 ***Plant material and sample generation***

490 *Nicotiana tabacum* plants were grown and transiently transformed according to
491 Sparkes *et al.* (2006) GFP-SKL (Sparkes *et al.*, 2003), YFPSKL (Mathur *et al.*, 2002)
492 and StCFP (Brandizzi *et al.*, 2002) constructs were infiltrated at 0.04 optical density.
493 Leaf samples (~5mm²) were taken from plants after 3-4 days expression and
494 incubated in 25µM latrunculin b for 60 minutes prior to imaging.

495

496 ***Confocal imaging and determination of organelle association and residency time***
497 ***with chloroplasts***

498 Triple imaging of peroxisomes (YFPSKL), Golgi (StCFP) and chloroplasts
499 (autofluorescence) in live tobacco epidermal pavement cells was done using multi-
500 tracking in line switching mode on a Zeiss LSM510 Meta confocal microscope. CFP
501 was excited with a 458-nm argon laser and YFP/ chloroplast autofluorescence with a
502 514nm laser, their emissions passed through a HFT 458/514 main dichroic beam
503 splitter and NFT 490 and NFT 595 secondary dichroic beam splitter, and detected
504 using 470-500nm, 530-600nm and 647-690nm filters respectively. All imaging was
505 carried out using a 63 x 1.4 Numerical Aperture (NA) oil immersion objective with a
506 scan speed of 1.94 frames per second. Peroxisomes / Golgi which were up to 1µm
507 from the chloroplasts (as monitored by the autofluorescent signal) were categorised as
508 residing next to chloroplasts. Residency time of peroxisomes and Golgi on
509 chloroplasts were analysed manually. Only those which resided next too (and could
510 move laterally over the surface of) the chloroplast for more than 3 seconds were
511 included in the statistical analysis.

512 Dual imaging of peroxisomes (GFPSKL) and chloroplasts (autofluorescence) was
513 carried out using multi-tracking in line switching mode on a Zeiss LSM510 Meta
514 confocal microscope. GFP was excited with a 488-nm argon laser and
515 autofluorescence with a 514nm laser, their emissions passed through a HFT 488/543
516 main dichroic beam splitter and NFT 515 and NFT 545 secondary dichroic beam
517 splitter, and detected using 505-530nm and 636-690nm filters respectively. All
518 imaging was carried out using a 63 x 1.4 NA oil immersion objective. Twenty single

519 scans of a 143 x 143 μm area were taken, and the number of chloroplasts with a
520 juxtaposed peroxisome in each image was counted.

521

522 ***Optical trapping setup and data generation***

523 Optical trapping was performed using a cw 1090 nm laser (SPI) focused using a x100,
524 oil immersion, NA 1.49 TIRF objective lens (Nikon). Here we assume the effective
525 NA of the objective lens for optical trapping approaches a value of 1.0. The
526 assumption is based upon comparison of escape force measurements made on 1.0 μm
527 diameter polystyrene beads to theoretical values calculated using an optical tweezers
528 computational toolbox (Nieminen et al., 2007). TIRF objectives are not commonly
529 used for optical tweezers. Mahamdeh *et al.* (2011) also indicate that spherical
530 aberrations arising from trapping in aqueous media will reduce the effective numerical
531 aperture.

532 TIRF used an excitation laser with 473 nm wavelength (Becker and Hickl) with a
533 maximum output power of 5 mW, coupled by an optical fibre to a Nikon TIRF
534 adapter system and attenuated by neutral density filters (2 and / or 8 dependent on the
535 level of GFP-SKL expression). Emitted fluorescent light was filtered using a long
536 pass filter for wavelength transmission above 505 nm and imaged using an electron-
537 multiplier charge-coupled device (Andor Ixon EMCCD). This allowed visualisation
538 of the excited GFPSKL probe and detection of chloroplast autofluorescence. Note,
539 that whilst the TIRF technique was employed to give significant improvement of
540 signal to noise, it is also likely that we are operating in a highly inclined illumination.

541 Custom LabVIEW® software (National Instruments) was used to control the EMCCD
542 camera (Andor), microscope stage (Marshauser) and a shutter, which blocked the
543 laser beam used for trapping. A LabVIEW® interface was used to synchronise the
544 timing of peroxisome capture, stage translation and peroxisome release over 110 or
545 229 frame videos; peroxisomes were monitored for 10 frames prior to trap activation,
546 40 frames upon trap activation prior to movement, 10 frames for the 6 μm translation,
547 10 frames after the translation, and 40 or 159 frames after the trap was deactivated
548 (relating to 5.3second or 21.5second recovery periods respectively). Stage translation
549 was measured to be 5.74 μm in 1 second with the EMCCD cycle time of 0.135
550 seconds giving approximately 7.5 frames per second. The video sequences were
551 stored as 16-bit stacked “tagged image file format” (tiff) files for subsequent analysis

552 of peroxisome behaviour. Note, the data sets generated for figure 2 are a combination
553 of the above trapping routine and an earlier version where trap shuttering was
554 manually controlled over a 70 frame video.

555

556 The minimal force (i.e. the escape force) required to trap peroxisomes, in a non-cp
557 environment, were measured by application of a viscous drag force (Supp Fig. 2). The
558 laser trap strength and viscous properties were investigated using a set of controlled
559 experiments where the stage velocity was varied. For each stage velocity, the laser
560 power required to keep 50% of the captured peroxisomes in the optical trap was
561 determined over a fixed $6\mu\text{m}$ translation distance (Supp Fig. 2). The fluorescent
562 organelles were observed under TIRF illumination. Due to variability in peroxisome
563 diameter it was necessary to measure 30-80 peroxisomes at each stage velocity to
564 obtain a representative laser power. Thus, the reported laser power is for an “average”
565 peroxisome (with plotted error bars indicating S.E uncertainty in laser power). The
566 viscous drag force for each stage velocity was calculated using Stokes’ law with an
567 assumed viscosity value of 0.06 Pa s (Scherp and Hasenstein, 2007) and the average
568 measured peroxisome diameter. Error bars for viscous drag force calculations used the
569 S.E. variation of peroxisome diameter. As a control, the same procedure was applied
570 to $1\mu\text{m}$ diameter polystyrene beads in water (0.00089 Pa s).

571

572 *Analysis of optical trapping data*

573 Trapping data from each repetition was normalised against differences in sample size
574 to determine the percentages of peroxisomes that were either trapped, untrapped or
575 which escaped the trap per leaf sample. The weighted mean values were taken of
576 these percentages for whole datasets and plotted. Between 36 and 62 peroxisomes in
577 total underwent the trapping protocol at any given laser trapping power resulting in
578 $n=338$ for chloroplast and $n=381$ for non-chloroplast associated total sample sizes.
579 These totals represent between 5 and 9 repetitions, where each repetition is from 1
580 leaf sample taken from 6 – 9 independent plants. Trapping was only attempted once
581 per peroxisome, repeated trapping of the same peroxisome was not undertaken.

582

583 Displacement values for peroxisome and peroxule dynamics were carried out using
584 ImageJ (NIH).

585

586 In order to gather statistically significant peroxisome motion data, we developed a
587 customized detection and tracking algorithm using a combination of python (scipy)
588 and custom written scripts and algorithms. The data were first filtered using the
589 Laplace-of-Gaussian scale-space method (Lindenberg 1994) to selectively filter for
590 objects in a given size range. Next, robust image statistics based thresholding (Median
591 Absolute Deviation) selected only salient objects in the resulting filtered data as
592 outlined in Murtagh *et al.* (2000). Object tracking was performed using a Global
593 Nearest Neighbours point registration approach, implemented as a modified version of
594 the Jonker-Volgenant linear assignment problem algorithm, altered to allow
595 rectangular cost matrices and cost cut-offs. In addition, sub-pixel peroxisome
596 positions were calculated using a filtered intensity weighted centroid function.
597 Tracking validation was performed by manual verification. The resulting trajectories
598 were then analysed to determine the peroxisome motion between the moment that the
599 optical trap was disengaged and the end of the recovery period.

600

601 Force calculations are described in the spring model (see supplementary note).

602

603

604 **Supplementary data**

605

606 **Supplementary Figure 1. Relationship between cp and non-cp peroxisomal**
607 **behaviour in the optical trap.**

608

609 **Supplementary Figure 2: Laser power required for trapping peroxisomes and**
610 **polystyrene beads at different stage velocities.**

611

612 **Supplementary Figure 3: Spring model definition.**

613

614 **Supplementary Figure 4: Example fits to the data using the simple spring model.**

615

616 **Supplementary Table 1: Relationship between optical laser trap power and**
617 **peroxule formation characteristics from cp and non-cp peroxisomes.**

618

619 **Supplementary Movie 1. Peroxisome association with chloroplasts**

620

621 **Supplementary Movie 2. Peroxisomes can be trapped and moved laterally within**
622 **tobacco leaf epidermal cells.**

623

624 **Supplementary Movie 3. Peroxisome behaviour in the optical trap under actin**
625 **depolymerisation.**

626

627 **Supplementary Note. Spring Model of Peroxisome Motion**

628

629 **Acknowledgements**

630 IS and HBG are funded by the BBSRC (BB/I006184/2) and an STFC user access
631 facility grant (LSP907), JM is funded by a Wellcome Trust Institutional Strategic
632 Support Award (WT097835MF) and NAT by The Leverhulme Trust and STFC. We
633 would like to thank Anne Kearns and Ian Leaves for technical assistance with
634 growing the tobacco plants required for the experiments, and to members of the plant
635 cell biology group at Oxford Brookes University for help with experimental logistics.
636 YFPSKL and StCFP were gifts from Prof. J. Mathur and Prof. C. Hawes respectively.
637

638 **Author contributions**

639 Experiments were conceived by IS and experimental data generated by HBG and IS.
640 ADW, SWB, BC and MRP built, customised, maintained and facilitated the use of the
641 optical trap-TIRF system. Experimental design was discussed with HBG, ADW,
642 SWB and JM. ADW calibrated the system and performed bead trapping experiments.
643 HBG performed all Image J analysis. JM wrote the tracking algorithm to generate the
644 displacement values for NAT. Visual confirmation of tracking was carried out by JM,
645 HBG and IS. NAT applied the simple model of a viscously-damped sphere on a
646 spring to determine the forces involved in the system. IS wrote the manuscript with
647 comments from all authors. NAT wrote the supplementary note section. NAT and
648 ADW were involved in writing the section relating to forces.

649

650 **Figure legends**

651

652 **Figure 1. Optical trapping and movement of peroxisomes away from**
653 **chloroplasts in tobacco leaf epidermal cells.**

654 Schematic representation of the trapping procedure (A-D) and the corresponding
655 micrographs (E-H) are shown. Upon turning the trap on (A,E) and moving the stage
656 $6\mu\text{m}$ at a set speed (B,F; referred to as translation period) the trapped peroxisome (p,
657 white arrow) is pulled away from the chloroplast (cp) and a peroxule (arrowhead) is
658 formed. Upon turning the trap off (C,G) the peroxisome recoils back towards its
659 original position next to the chloroplast (D,H). Peroxisome displacement during the
660 recovery period (referred to as recovery displacement) is measured (double
661 arrowhead). Asterisk denotes the tip of the peroxule. Scale bar $6\mu\text{m}$.

662

663 **Figure 2. Higher optical trapping laser power is required to trap and move**
664 **peroxisomes away from chloroplasts.**

665 Non-cp (A) and Cp (B) associated peroxisomes underwent the optical trapping
666 protocol using various trapping laser powers and their trapping characteristics were
667 scored; remained in the trap over the $6\mu\text{m}$ translation (black bar A,B), unable to be
668 trapped (white bar A,B) or escaped the trap during the translation (grey bar A,B).
669 Percentages displayed are based on weighted means from a set of independent
670 experiments. Supp Figure 1 compares cp with non-cp for all three trapping categories
671 and indicates significant differences between peroxisomes that are trapped or escape
672 from the trap for cp versus non-cp. Relationship between optical laser trap power and
673 peroxule formation are given in Supp table 1.

674 Stills from Supp movie 3C-E representing before and after translation events for
675 peroxisomes which are trapped, not trapped or escape the trap during the translation
676 event are displayed (C, arrowhead). Note, peroxisomes not subjected to trapping in
677 the same cell are shown for comparison (arrow). The translation event is based on
678 movement of the stage and not the trap. Composite image of frames captured during
679 the translation event show that the trapped peroxisome does not appear to move
680 whereas organelles that escape the trap or are not trapped result in comet like tails
681 (merged panels). Scale bar $6\mu\text{m}$.

682

683 **Figure 3. Correlation between peroxisome displacement during the recovery**
684 **period and peroxule tip displacement during translation indicates anchored**
685 **tethering between chloroplasts and peroxisomes.**

686 Peroxule tip displacement during the translation period was plotted against the
687 peroxisome displacement during the recovery period for chloroplast associated (A;
688 $n=37$) and non associated peroxisomes (B; $n=46$). Peroxisomes were trapped with
689 37mW optical trap laser power followed by a 21.5 second recovery period. The
690 behaviour of cp samples is indicative of anchored tethers where the peroxule tip
691 represents the base of the tether: small peroxule tip displacement combined with large
692 peroxisome recovery displacement (circle). Note, the sample sizes are different to
693 those in supplementary table 1 as displacement could only be measured if the
694 peroxule was observable for the entire period.

695

696 **Figure 4. Cumulative distribution functions of model parameters for cp and non-**
697 **cp associated peroxisomes.**

698 Recovery displacement b is larger for cp than non-cp peroxisomes (A), whereas k/μ
699 values, indicative of the tether stiffness, are broadly similar (B). Also, shown are the
700 derived spring constants (C) and initial recovery forces (D) calculated assuming a
701 viscosity of 0.06 Pa s for the cytoplasm. Values are derived using the spring model
702 described in the supplementary information alongside Supp Fig 2-4.

703

704 **Supplementary material**

705

706 **Supplementary Movie 1. Peroxisome association with chloroplasts.**

707 Time lapse images were taken of peroxisomes (green), Golgi (cyan) and chloroplasts
708 (magenta) in tobacco leaf epidermal cells. Organelles were visualised through
709 transient expression of fluorescent fusions (YFPSKL for peroxisomes and STCFP for
710 Golgi bodies) or autofluorescence (chloroplasts). Compared to Golgi, peroxisomes
711 spend longer periods of time associated with chloroplasts. The peroxisome appears
712 tethered to a fixed zone on the surface of the chloroplast as the chloroplast moves (A),
713 and in some cases the peroxisomes can also move laterally over the surface (B). Scale
714 bar 5 μm .

715

716 **Supplementary Movie 2. Peroxisomes can be trapped and moved laterally within**
717 **tobacco leaf epidermal cells.**

718 Peroxisomes were trapped (arrowhead) and the stage moved 6 μm horizontally.
719 During the translation peroxisomes either escaped the trap (A,C) or were moved 6 μm
720 (B,D). Upon turning the trap off the peroxisomes moved back towards their original
721 position (B,D). Peroxisomes juxtaposed to chloroplasts (C,D) behaved similarly to
722 peroxisomes which were not (A,B). In both cases, peroxules were observed (B,D)
723 Scale bar 6 μm .

724

725 **Supplementary Movie 3. Peroxisome behaviour in the optical trap under actin**
726 **depolymerisation.**

727 A trapped non-cp (A) and cp (B) peroxisome undergoes the 6 μm translation resulting
728 in peroxule formation. Upon turning the trap off the peroxisome moves back along the
729 length of the peroxule. Movies highlighting examples of non-cp peroxisomes in
730 tobacco leaf epidermal cells which are either (C) trapped, (D) not trapped (E) or
731 escape the trap over the translation period. The samples were treated with latrunculin
732 B and so any subsequent motion upon turning the trap off is independent of acto-
733 myosin. Scale Bar 6 μm . Arrow head denotes peroxisome undergoing the trapping
734 routine.

735

736

Parsed Citations

- Andersson, MX., Goksor, M., and Sandelius, AS. (2007)** Optical manipulation reveals strong attracting forces at membrane contact sites between endoplasmic reticulum and chloroplasts. *J. Biol. Chem.* 282:1170-1174.
Pubmed: [Author and Title](#)
CrossRef: [Author and Title](#)
Google Scholar: [Author Only](#) [Title Only](#) [Author and Title](#)
- Asada, K. (2006)** Production and scavenging of reactive oxygen species in chloroplasts and their functions. *Plant Physiol.* 141:391-396.
Pubmed: [Author and Title](#)
CrossRef: [Author and Title](#)
Google Scholar: [Author Only](#) [Title Only](#) [Author and Title](#)
- Avisar, D., Prokhnevsky, Al., Makarova, KS., Koonin, EV., and Dolja, VV. (2008)** Myosin XI-K Is required for rapid trafficking of Golgi stacks, peroxisomes, and mitochondria in leaf cells of *Nicotiana benthamiana*. *Plant Physiol.* 146:1098-1108.
Pubmed: [Author and Title](#)
CrossRef: [Author and Title](#)
Google Scholar: [Author Only](#) [Title Only](#) [Author and Title](#)
- Barton, K., Mathur, N., and Mathur, J. (2013)** Simultaneous live-imaging of peroxisomes and the ER in plant cells suggests contiguity but no luminal continuity between the two organelles. *Front. Physiol.* 4:196. doi: 10.3389/fphys.2013.00196.
Pubmed: [Author and Title](#)
CrossRef: [Author and Title](#)
Google Scholar: [Author Only](#) [Title Only](#) [Author and Title](#)
- Brandizzi F., Snapp EL., Roberts AG., Lippincott-Schwartz J., Hawes C. (2002)** Membrane protein transport between the endoplasmic reticulum and the Golgi in tobacco leaves is energy dependent but cytoskeleton independent. *Plant Cell* 14:1293-1309.
Pubmed: [Author and Title](#)
CrossRef: [Author and Title](#)
Google Scholar: [Author Only](#) [Title Only](#) [Author and Title](#)
- Buchnik, L., Abu-Abied, M., and Sadot, E. (2015)** Role of plant myosins in motile organelles: Is a direct interaction required? *Journal of integrative plant biology* 57:23-30.
Pubmed: [Author and Title](#)
CrossRef: [Author and Title](#)
Google Scholar: [Author Only](#) [Title Only](#) [Author and Title](#)
- Bussell, J.D., Behrens, C., Ecke, W., and Eubel, H. (2013)** Arabidopsis peroxisome proteomics. *Front. Plant Sci.* 4:101. doi: 10.3389/fpls.2013.00101
Pubmed: [Author and Title](#)
CrossRef: [Author and Title](#)
Google Scholar: [Author Only](#) [Title Only](#) [Author and Title](#)
- Cutler, SR., Ehrhardt, DW., Griffiths, JS., and Somerville, CR. (2000)** Random GFP::cDNA fusions enable visualization of subcellular structures in cells of *Arabidopsis* at a high frequency. *PNAS* 97:3718-3723.
Pubmed: [Author and Title](#)
CrossRef: [Author and Title](#)
Google Scholar: [Author Only](#) [Title Only](#) [Author and Title](#)
- Desai M, Hu J. (2008)** Light induces peroxisome proliferation in *Arabidopsis* seedlings through the photoreceptor phytochrome A, the transcription factor HY5 HOMOLOG, and the peroxisomal protein PEROXIN11b. *Plant Physiol.* 146:1117-27.
Pubmed: [Author and Title](#)
CrossRef: [Author and Title](#)
Google Scholar: [Author Only](#) [Title Only](#) [Author and Title](#)
- Frederick, SE., and Newcomb, EH. (1969).**Microbody-like organelles in leaf cells. *Science* 163:1353-1355
Pubmed: [Author and Title](#)
CrossRef: [Author and Title](#)
Google Scholar: [Author Only](#) [Title Only](#) [Author and Title](#)
- Hammer, JA, 3rd, and Sellers, JR. (2012)** Walking to work: roles for class V myosins as cargo transporters. *Nat. Rev. Mol. Cell Biol.* 13:13-26.
Pubmed: [Author and Title](#)
CrossRef: [Author and Title](#)
Google Scholar: [Author Only](#) [Title Only](#) [Author and Title](#)
- Hanson, MR., and Sattarzadeh, A.(2013).**Trafficking of proteins through plastid stromules. *Plant Cell* 25: 2774-2782.
Pubmed: [Author and Title](#)
CrossRef: [Author and Title](#)
Google Scholar: [Author Only](#) [Title Only](#) [Author and Title](#)
- Higa T, Suetsugu N, Kong SG, Wada M. (2014)** Actin-dependent plastid movement is required for motive force generation in directional nuclear movement in plants. *PNAS* 111:4327-31.
Pubmed: [Author and Title](#)
CrossRef: [Author and Title](#)
Google Scholar: [Author Only](#) [Title Only](#) [Author and Title](#)
- Hu, J., Baker, A, Bartel, B., Linka, N., Mullen, RT., Reumann, S., and Zolman, BK. (2012)** Plant peroxisomes: biogenesis and

function. Plant Cell 24: 2279-2303.

Pubmed: [Author and Title](#)
CrossRef: [Author and Title](#)
Google Scholar: [Author Only](#) [Title Only](#) [Author and Title](#)

Jedd, G., and Chua, NH. (2002) Visualization of peroxisomes in living plant cells reveals acto-myosin-dependent cytoplasmic streaming and peroxisome budding. Plant Cell Physiol. 43:384-392.

Pubmed: [Author and Title](#)
CrossRef: [Author and Title](#)
Google Scholar: [Author Only](#) [Title Only](#) [Author and Title](#)

Knoblach, B., Sun, X., Coquelle, N., Fagarasanu, A., Poirier, RL., and Rachubinski, RA (2013) An ER-peroxisome tether exerts peroxisome population control in yeast. EMBO J. 32: 2439-2453.

Pubmed: [Author and Title](#)
CrossRef: [Author and Title](#)
Google Scholar: [Author Only](#) [Title Only](#) [Author and Title](#)

Lindeberg T. (1994) Scale-space theory in computer vision. eds Kluwer Academic Publishers, Boston.

Pubmed: [Author and Title](#)
CrossRef: [Author and Title](#)
Google Scholar: [Author Only](#) [Title Only](#) [Author and Title](#)

Madison, SL., and Nebenführ, A. (2013). Understanding myosin functions in plants: are we there yet? Curr. Opin. Plant. Biol. 16:710-717

Pubmed: [Author and Title](#)
CrossRef: [Author and Title](#)
Google Scholar: [Author Only](#) [Title Only](#) [Author and Title](#)

Mahamdeh M, Campos CP., Schäffer E. (2011) Under-filling trapping objectives optimizes the use of the available laser power in optical tweezers. Opt. Express 19:11759-11768.

Pubmed: [Author and Title](#)
CrossRef: [Author and Title](#)
Google Scholar: [Author Only](#) [Title Only](#) [Author and Title](#)

Mano, S., Nakamori, C., Hayashi, M., Kato, A., Kondo, M., and Nishimura, M. (2002) Distribution and characterization of peroxisomes in Arabidopsis by visualization with GFP: dynamic morphology and actin-dependent movement. Plant Cell Physiol. 43:331-341.

Pubmed: [Author and Title](#)
CrossRef: [Author and Title](#)
Google Scholar: [Author Only](#) [Title Only](#) [Author and Title](#)

Mathur, J., Barton KA, Schattat, MH. (2013) Fluorescent Protein Flow within Stromules Plant Cell 25: 2771-2772.

Pubmed: [Author and Title](#)
CrossRef: [Author and Title](#)
Google Scholar: [Author Only](#) [Title Only](#) [Author and Title](#)

Mathur, J., Mammone, A, and Barton, KA (2012) Organelle extensions in plant cells. J. Integr. Plant. Biol. 54, 851-867

Pubmed: [Author and Title](#)
CrossRef: [Author and Title](#)
Google Scholar: [Author Only](#) [Title Only](#) [Author and Title](#)

Mathur, J., Mathur, N., and Hulskamp, M. (2002) Simultaneous visualization of peroxisomes and cytoskeletal elements reveals actin and not microtubule-based peroxisome motility in plants. Plant Physiol. 128:1031-1045

Pubmed: [Author and Title](#)
CrossRef: [Author and Title](#)
Google Scholar: [Author Only](#) [Title Only](#) [Author and Title](#)

Mehrshahi, P., Stefano, G., Andaloro, JM., Brandizzi, F., Froehlich, JE., DellaPenna, D. (2013) Transorganellar complementation redefines the biochemical continuity of endoplasmic reticulum and chloroplasts. PNAS 110:12126-12131

Pubmed: [Author and Title](#)
CrossRef: [Author and Title](#)
Google Scholar: [Author Only](#) [Title Only](#) [Author and Title](#)

Murtagh F, Starck JL. (2000) Image processing through multiscale analysis and measurement noise modeling. Stat. Comput. 10:95-103.

Pubmed: [Author and Title](#)
CrossRef: [Author and Title](#)
Google Scholar: [Author Only](#) [Title Only](#) [Author and Title](#)

Nieminen TA, Loke VLY., Stilgoe AB., Knoner G., Branczyk AM. (2007) Optical tweezers computational toolbox. J. Opt. Pure Appl. Opt. 9:S196-S203.

Pubmed: [Author and Title](#)
CrossRef: [Author and Title](#)
Google Scholar: [Author Only](#) [Title Only](#) [Author and Title](#)

Oikawa, K., Kasahara, M., Kiyosue, T., Kagawa, T., Suetsugu, N., Takahashi, F., Kanegae, T., Niwa, Y., Kadota, A., and Wada, M. (2003) Chloroplast unusual positioning1 is essential for proper chloroplast positioning. Plant Cell 15:2805-2815.

Pubmed: [Author and Title](#)
CrossRef: [Author and Title](#)
Google Scholar: [Author Only](#) [Title Only](#) [Author and Title](#)

Oikawa, K., Matsunaga, S., Mano, S., Kondo, M., Yamada, K., Hayashi, M., Kagawa, T., Kadota, A., Sakamoto, W., Higashi, S.,

- Watanabe, M., Mitsui, T., Shigemasa, A., Iino, T., Hosokawa, Y., Nishimura, M. (2015) Physical interaction between peroxisome and chloroplasts elucidated by in situ laser analysis. *Nature Plants* 1:15035 doi:10.1038/nplants.2015.35**
Pubmed: [Author and Title](#)
CrossRef: [Author and Title](#)
Google Scholar: [Author Only](#) [Title Only](#) [Author and Title](#)
- Oikawa, K., Yamasato, A., Kong, S., Kasahara, M., Nakia, M., Takahashi, F., Ogura, Y., Kagawa, T., Wada, M. (2008) Chloroplast outer envelope protein CHUP1 is essential for chloroplast anchorage to the plasma membrane and chloroplast movement. *Plant Physiology* 148:829-842**
Pubmed: [Author and Title](#)
CrossRef: [Author and Title](#)
Google Scholar: [Author Only](#) [Title Only](#) [Author and Title](#)
- Prestele, J., Hierl, G., Scherling, C., Hetkamp, S., Schwachheimer, C., Isono, E., Weckwerth, W., Wanner, G., and Gietl, C. (2010) Different functions of the C3HC4 zinc RING finger peroxins PEX10, PEX2, and PEX12 in peroxisome formation and matrix protein import. *PNAS* 107:14915-14920**
Pubmed: [Author and Title](#)
CrossRef: [Author and Title](#)
Google Scholar: [Author Only](#) [Title Only](#) [Author and Title](#)
- Prinz, WA (2014) Bridging the gap: membrane contact sites in signaling, metabolism, and organelle dynamics. *J. Cell Biol.* 205:759-769.**
Pubmed: [Author and Title](#)
CrossRef: [Author and Title](#)
Google Scholar: [Author Only](#) [Title Only](#) [Author and Title](#)
- Sandalio, L.M. and Romero-Puertas, M.C. (2015) Peroxisomes sense and respond to environmental cues by regulating ROS and RNS signalling networks. *Annals of Botany* 116:475-485**
Pubmed: [Author and Title](#)
CrossRef: [Author and Title](#)
Google Scholar: [Author Only](#) [Title Only](#) [Author and Title](#)
- Schattat, M., Barton, K., Baudisch, B., Klosgen, RB., and Mathur, J. (2011) Plastid stromule branching coincides with contiguous endoplasmic reticulum dynamics. *Plant Physiol.* 155:1667-1677.**
Pubmed: [Author and Title](#)
CrossRef: [Author and Title](#)
Google Scholar: [Author Only](#) [Title Only](#) [Author and Title](#)
- Scherp, P., and Hasenstein, KH. (2007) Anisotropic viscosity of the Chara (Characeae) rhizoid cytoplasm. *Am. J. Bot.* 94:1930-1934.**
Pubmed: [Author and Title](#)
CrossRef: [Author and Title](#)
Google Scholar: [Author Only](#) [Title Only](#) [Author and Title](#)
- Schmidt von Braun, S., and Schleiff, E. (2008) The chloroplast outer membrane protein CHUP1 interacts with actin and profilin. *Planta* 227:1151-1159**
Pubmed: [Author and Title](#)
CrossRef: [Author and Title](#)
Google Scholar: [Author Only](#) [Title Only](#) [Author and Title](#)
- Schnarrenberger, C., and Burkhard, C. (1977) In-vitro interaction between chloroplasts and peroxisomes as controlled by inorganic phosphate. *Planta* 134:109-114.**
Pubmed: [Author and Title](#)
CrossRef: [Author and Title](#)
Google Scholar: [Author Only](#) [Title Only](#) [Author and Title](#)
- Schumann, U., Prestele, J., O'Geen, H., Brueggeman, R., Wanner, G., and Gietl, C. (2007) Requirement of the C3HC4 zinc RING finger of the Arabidopsis PEX10 for photorespiration and leaf peroxisome contact with chloroplasts. *PNAS* 104:1069-1074**
Pubmed: [Author and Title](#)
CrossRef: [Author and Title](#)
Google Scholar: [Author Only](#) [Title Only](#) [Author and Title](#)
- Scott, I., Sparkes, IA, and Logan, DC. (2007) The missing link: inter-organellar connections in mitochondria and peroxisomes? *Trends Plant Sci.* 12:380-381.**
Pubmed: [Author and Title](#)
CrossRef: [Author and Title](#)
Google Scholar: [Author Only](#) [Title Only](#) [Author and Title](#)
- Sinclair, AM., Trobacher, CP., Mathur, N., Greenwood, JS., Mathur, J. (2009) Peroxule extension over ER-defined paths constitutes a rapid subcellular response to hydroxyl stress. *Plant J.* 59:231-242**
Pubmed: [Author and Title](#)
CrossRef: [Author and Title](#)
Google Scholar: [Author Only](#) [Title Only](#) [Author and Title](#)
- Sparkes, I (2011) Recent advances in understanding plant myosin function: Life in the fast lane. *Mol Plant* 4:805-812**
Pubmed: [Author and Title](#)
CrossRef: [Author and Title](#)
Google Scholar: [Author Only](#) [Title Only](#) [Author and Title](#)
- Sparkes IA, Brandizzi F, Slocombe SP, El-Shami M, Hawes C, Baker A (2003) An Arabidopsis pex10 null mutant is embryo lethal, implicating peroxisomes in an essential role during plant embryogenesis. *Plant Physiol.* 133:1809-1819.**

Pubmed: [Author and Title](#)
CrossRef: [Author and Title](#)
Google Scholar: [Author Only](#) [Title Only](#) [Author and Title](#)

Sparkes, IA, Ketelaar, T., de Ruijter, NC., and Hawes, C. (2009b) Grab a Golgi: laser trapping of Golgi bodies reveals in vivo interactions with the endoplasmic reticulum. Traffic 10:567-571.

Pubmed: [Author and Title](#)
CrossRef: [Author and Title](#)
Google Scholar: [Author Only](#) [Title Only](#) [Author and Title](#)

Sparkes, IA, Teanby, NA, and Hawes, C. (2008) Truncated myosin XI tail fusions inhibit peroxisome, Golgi, and mitochondrial movement in tobacco leaf epidermal cells: a genetic tool for the next generation. J. Exp. Bot. 59:2499-2512.

Pubmed: [Author and Title](#)
CrossRef: [Author and Title](#)
Google Scholar: [Author Only](#) [Title Only](#) [Author and Title](#)

Sparkes I., Runions, J., Hawes, C., Griffing L. (2009a) Movement and remodelling of the Endoplasmic Reticulum in nondividing cell sof tobacco leaves. Plant Cell 21:3937-3949.

Pubmed: [Author and Title](#)
CrossRef: [Author and Title](#)
Google Scholar: [Author Only](#) [Title Only](#) [Author and Title](#)

Sparkes IA, Runions J., Kearns A, Hawes C. (2006) Rapid, transient expression of fluorescent fusion proteins in tobacco plants and generation of stably transformed plants. Nat. Protoc. 1:2019-2025.

Pubmed: [Author and Title](#)
CrossRef: [Author and Title](#)
Google Scholar: [Author Only](#) [Title Only](#) [Author and Title](#)

Stefano, G., Hawes, C., and Brandizzi, F. (2014) ER - the key to the highway. Curr. Opin. Plant Biol. 22:30-38.

Pubmed: [Author and Title](#)
CrossRef: [Author and Title](#)
Google Scholar: [Author Only](#) [Title Only](#) [Author and Title](#)

Tamura K, Iwabuchi K, Fukao Y, Kondo M, Okamoto K, Ueda H, Nishimura M, Hara-Nishimura I. (2013) Myosin XI-i links the nuclear membrane to the cytoskeleton to control nuclear movement and shape in Arabidopsis. Curr. Biol. 23:1776-81.

Pubmed: [Author and Title](#)
CrossRef: [Author and Title](#)
Google Scholar: [Author Only](#) [Title Only](#) [Author and Title](#)

Thazar-Poulot N, Miquel M, Fobis-Loisy I, Gaude T (2015) Peroxisome extensions deliver the Arabidopsis SDP1 lipase to oil bodies. PNAS 112:4158-63

Pubmed: [Author and Title](#)
CrossRef: [Author and Title](#)
Google Scholar: [Author Only](#) [Title Only](#) [Author and Title](#)

Yang, Y., Sage, TL., Liu, Y., Ahmad, TR., Marshall, WF., Shiu, SH., Froehlich, JE., Imre, KM., and Osteryoung, KW. (2011) CLUMPED CHLOROPLASTS 1 is required for plastid separation in Arabidopsis. PNAS 108:18530-18535.

Pubmed: [Author and Title](#)
CrossRef: [Author and Title](#)
Google Scholar: [Author Only](#) [Title Only](#) [Author and Title](#)